Proceedings of the 7th International Symposium on Cavitation
CAV2009 – Paper No. 113
August 17-22, 2009, Ann Arbor, Michigan, USA

Blade load dynamics in cavitating and two phase flows

Morten Kjeldsen
Norwegian University of Science and Technology
Trondheim, Norway

Roger E. A. Arndt
University of Minnesota
Minneapolis, MN, Minnesota

ABSTRACT

A comparative study of lift dynamics on a hydrofoil and inlet pressure dynamics on a pump impeller vane is described in this paper. The hydrofoil, a rectangular planform NACA 0015 with a chord length of c=0.081m, fitted with a special arrangement that allowed the injection of gas downstream of the minimum pressure point, was tested in the St Anthony Falls Laboratory (SAFL) closed loop water tunnel at the University of Minnesota. The SAFL water tunnel is specially suited for gas injection type measurements due to high gas removal capabilities. The tests on the hydrofoil also included a full range of cavitation experiments. The pump tests were made at the Waterpower Laboratory at the Norwegian University of Science and Technology (NTNU). Upstream of the pump inlet a special bubble injection device was located. This arrangement allows a controlled amount of gas to enter the flow. The water and gas flow rates were measured separately. Lift measurements from the hydrofoil study display a striking similarity between gas loaded and cavitation lift dynamics. The pump dynamics data show a maximum for a moderate gas void fraction. It is also observed that a more pronounced low frequency dynamics is present for the gas-loaded systems.

INTRODUCTION

This paper draws on the experience authors have had during research collaboration on various aspects of cavitation dynamics on hydrofoils that spans a ten-year period dating back to 1998. One remarkable feature of hydrofoil cavitation dynamics is that high, and sustained, levels of lift oscillations can be observed for moderate cavitation numbers where partial cavitation occurs. Numerical simulations and a range of experiments indicate that the oscillations are related to the shedding of vortical clouds of bubbles into the wake. Some performance breakdown is observed at this stage, but total performance breakdown doesn't take place until supercavitation occurs. At this stage in cavitation behavior, both noise and vibration are at diminished levels.

Recently an interest in two phase flows led to the question of whether gaseous cavitation would show, at least qualitatively, the same lift dynamics at moderate gas loads as is experienced with cavitation. One motivation for the current study is the reliability of flow systems that may operate in a two-phase regime. Of special interest are submerged installations that are made compact in order to make them economically feasible for offshore installations. By making systems compact the separation efficiencies are more likely less than those on analogous land based plants. It is also likely that submerged flow systems designed for single-phase operation can experience periods of two-phase flow due to gas load. If this gas load can increase dynamics, fatigue loads can occur and hence result in a less reliable system. Our approach to the study of gas load induced dynamics utilize a combination of hydrofoil observations in a water tunnel, numerical analysis, observations of flow in an instrumented centrifugal pump. This paper addresses the experimental part of the program.

The authors are aware of studies made on pump performance for gas loaded pumps focusing on performance characteristics; i.e. global parameters. Literature on experimental works on local phenomena within the pump impeller seems however to be scarce. The role of gas in liquids in conjunction with flow induced vibration is a topic of interest for many areas of engineering. English [5] has e.g. presented a study on ship vibration when injecting air in the propeller stage.

EXPERIMENTAL SET UP

The experiments were performed with a 190mm span, 81 mm chord foil having a NACA 0015 cross section. The foil was configured to allow the injection of gas (air) close to the leading edge, see Figure 1 for details. Most of the experimental data were collected at a flow velocity of about 8m/s and at test section pressures up to 2 bar, i.e. a cavitation index above 6. Gas load experiments were performed at different test section pressures. The experiments were made in the SAFL high-speed water tunnel that is ideally suited to this project because of the

ability to remove large quantities of air during operation. Recent experience with similar experiments on the use of ventilation for drag reduction on hydrofoils left much of the infrastructure/ instrumentation necessary easily available. More details on the experimental set up can be found in e.g. Kopriva et al [4].

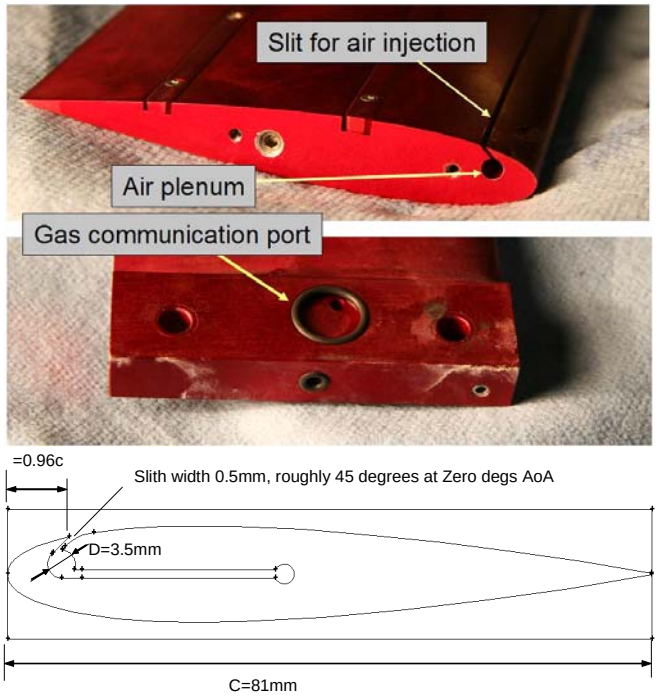

Figure 1: Photos and design details of the NACA 0015 hydrofoil used in the ventilation studies.

A standard centrifugal pump with no special design features to improve performance under two-phase load conditions was installed in a test rig at NTNU Vannkraftlaboratoriet (the Hydropower Lab). The pump was connected at both the inlet and the outlet to a permanent pressure vessel and was operated in a closed loop by throttling, using a valve on the delivery side of the pump. Comparative experiments consisted of constant throttling (valve position) at the same rotational speed but various gas void fractions. The closed loop arrangement made it possible to make a variation of the inlet pressure in the range 2 to 5 bars. Adjustment of pressure was done by evacuating/pressurizing air within the permanent pressure vessel.

At the inlet section a bubble injection device was attached, 500mm upstream the inlet section, into which the total airflow rate could be controlled, see Figure 2. Bubbles were injected through a number of drilled holes/ports (1mm) in small cylindrical pipes protruding the pipe inlet section diameter, ID350mm. The flow was locally accelerated over the injection ports. The expected bubble sizes can be calculated using the theory of Silberman [2], see Equation 1. Between the injection device and the pump a segment of a transparent acrylic pipe segment was installed allowing the observation of the two phase flow.

$$D_{\max} = 2.4\sqrt{\frac{Q_{Gas,Injec}}{U_{liq}}} \qquad \textbf{Equation 1}$$

$$Q_{Gas,Injec} = \frac{Q_{Gas}}{N_{Exit}}$$

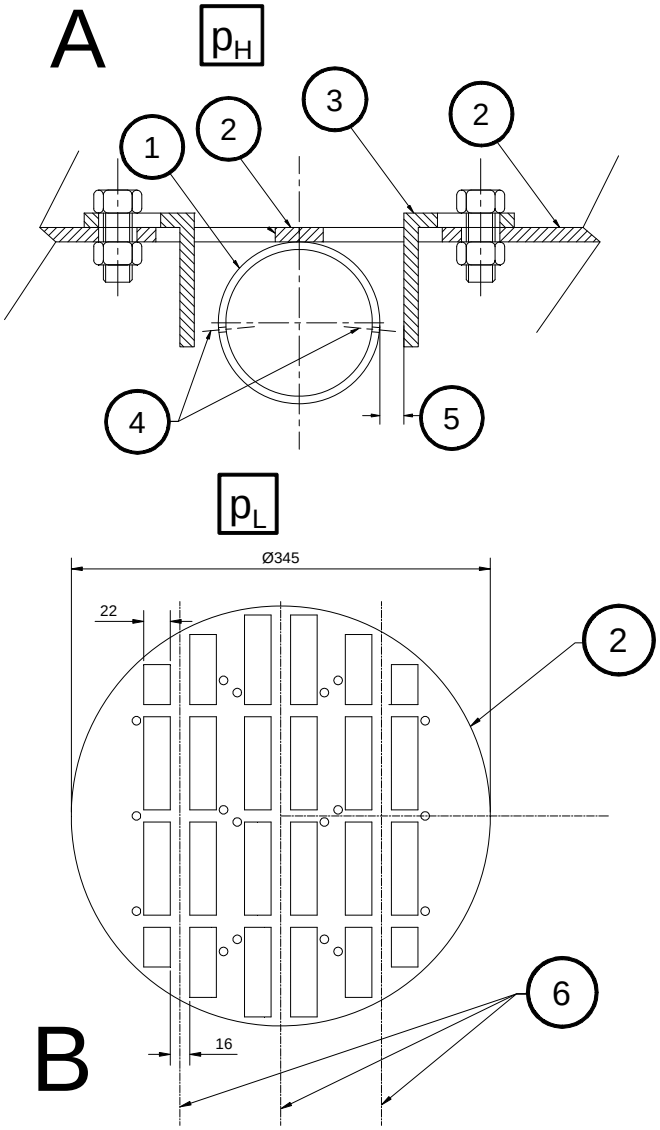

Figure 2 : Details of gas injection device utilized in pump gas injection studies. Flow from high pressure (pH) to low pressure (pL) through (adjustable size) gaps (5). Gaps (5) in cover plate (2), resting on injection pipes (1), can take different values by moving the slit adjustment piece (3). Center lines (6) of the injection pipes relative the cover (2) is shown in B. Injection ports (4) 1mm at -5 and 185 degrees and space 10 mm apart in the axial direction.

The inlet section of the impeller blade was equipped with two pressure transducers (Kulite LL80) flush mounted on the suction side, see **Figure 3.** The excitation voltage was equipped by on-board batteries and the measured transducer voltage

signal was transferred wirelessly with a (ST-500e Transmitter/SR-500 Receiver from Summation Research Inc) device enabling a transfer rate of 2000 samples per second per channel. The pump shaft is also equipped with a torque and speed measurement device (HBM T10F). The pump head was measured using a differential pressure transducer, making the geostatic level for measurement of inlet and outlet pressures equal. The liquid flow rate was measured using an electromagnetic flow meter upstream the bubble injection device, while the gas flow rate was monitored using a rotameter. All data, except the rotameter readings, was acquired using hardware from National Instruments (NI), and processed using LabView from NI.

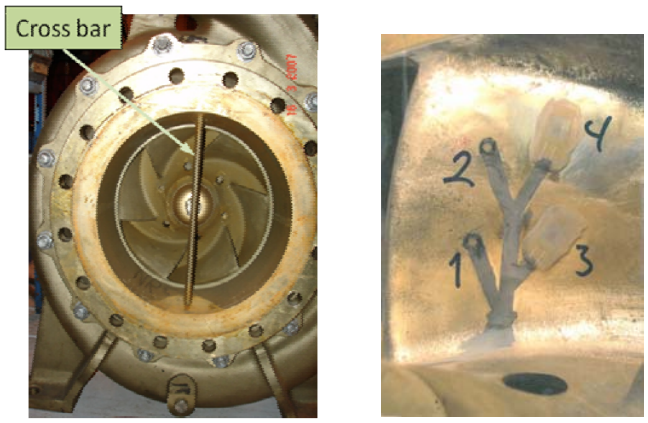

Figure 3 : Photos of pump and instrumentation of pump suction side impeller blade. Positions 1 and 2, left picture, indicate Kulite pressure transducers, 3 and 4 are strain gauges for which results are not reported in this study. The inlet diameter, upstream pipe attachment, of the pump is 350 mm.

RESULTS

Figure 4 shows the comparison between dynamics of a ventilated foil, as depicted in Figure 1, and a plain cavitating hydrofoil. The density ratio of injected gas and water is of interest, and Figure 5 gives lift characteristics both average and dynamics for various test section pressures. It should be noted that the authors, see Kjeldsen et al [1], found that there is a linear relationship between $\sigma_{vent}/2\alpha$ and $Q_{red,mod}$ the way they are defined herein.

The pump efficiency for single-phase conditions is given in Figure 6. The operation points, or single-phase flow rates, correspond to those where pressure dynamics has been observed for various gas void fractions. Figure 7 summarizes the observed pressure dynamics on transducer 1 for the selected pump operation points. For the pump it was also of great interest to observe dynamics for various gas-water ratios. Figure 8 gives the observed pressure dynamics for a range of inlet pressures. Note that the pump was not run at cavitation conditions.

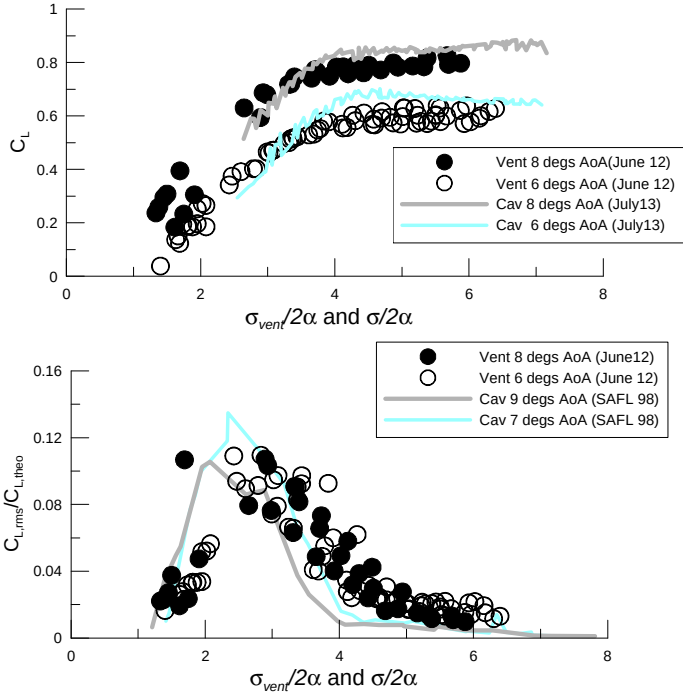

Figure 4: Comparison of experimental steady and unsteady characteristics for ventilated and cavitating flows using the cavity index based on cavity pressure. Note that for cavitation the cavity pressure is constant and equal to the vapor pressure for the given temperature. Previous data on cavitation lift dynamics has been used for comparison since many of the cavitation experiments in the current study were obscured by a oscillation lock-in between the lift balance and the cavitation shedding dynamics in the current experiments.

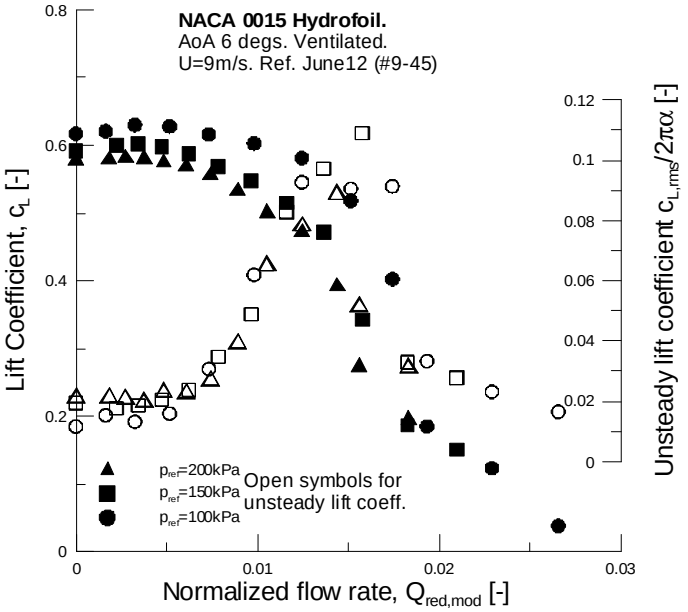

Figure 5: Lift performance and dynamics for ventilated hydrofoil for various test section pressures.

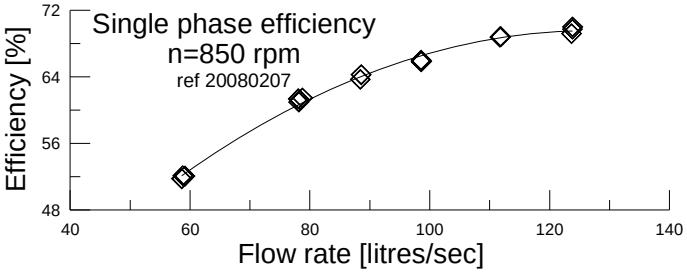

Figure 6 : Pump efficiencies for operation points, in term of flow rate, tested for impeller dynamics.

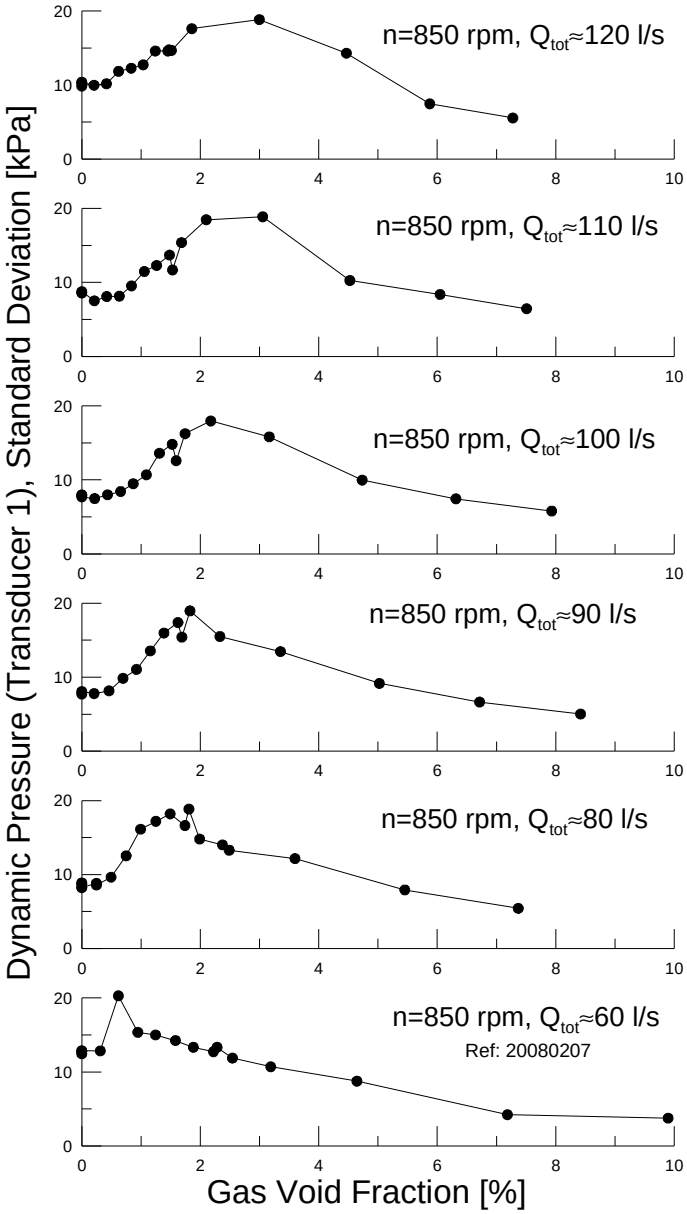

Figure 7: Dynamics as measured with suction side impeller blade transducer number 1, see Figure 3, and for an inlet/suction pressure of 3 bars (absolute).

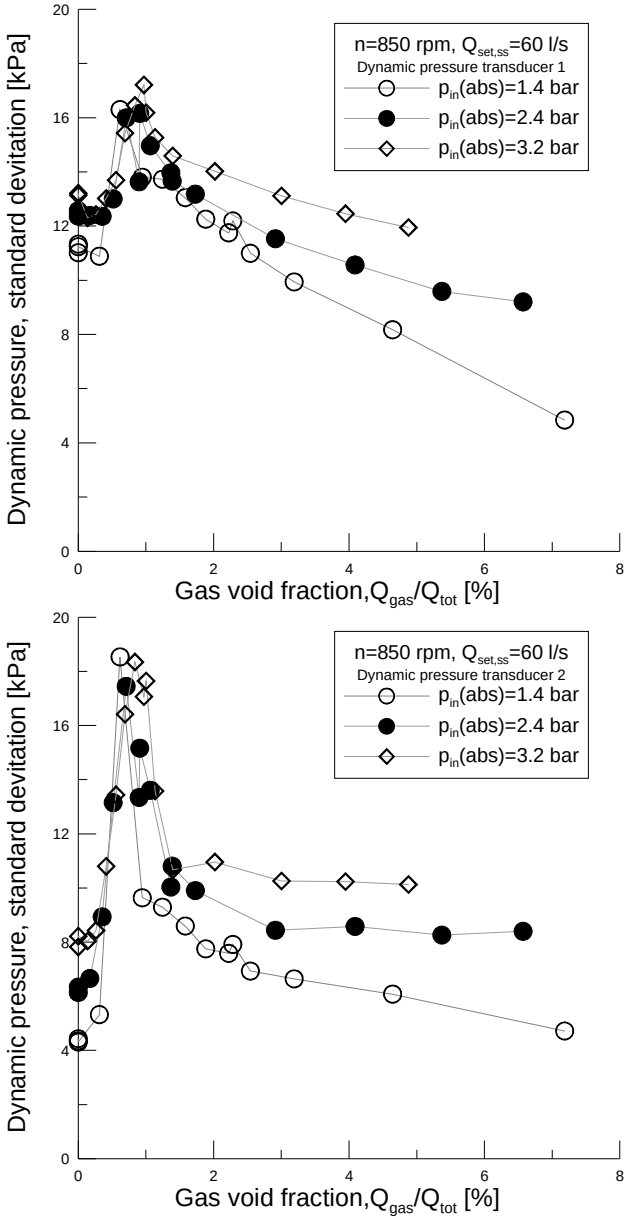

Figure 8: Pressure dynamics, given as standard devitation, on the impeller inlet of the pump tested in this study. Analysis is based on analysis of data low-pass filtered at 100Hz (i.e. roughly 7x the rotational speed).

Figure 4 through Figure 8 give the dynamics as a statistical quantity, i.e. standard deviations. Standard spectrum analyses have also been made of the situations considered. The original time series contain 16384 samples at 1000 samples per second (hydrofoil) and 2000 samples per second (pump). Figure 9 gives the analysis of the hydrofoil wing dynamic for both ventilation and cavitation, while Figure 10 given that for the gas loaded pump. A low pass filter, at 100 Hz or about 7x the rotational speed, have been used before the spectrum analysis. In addition the spectrum, as shown, is an average of 4 spectra from splitting the original time series into 4 independent segments.

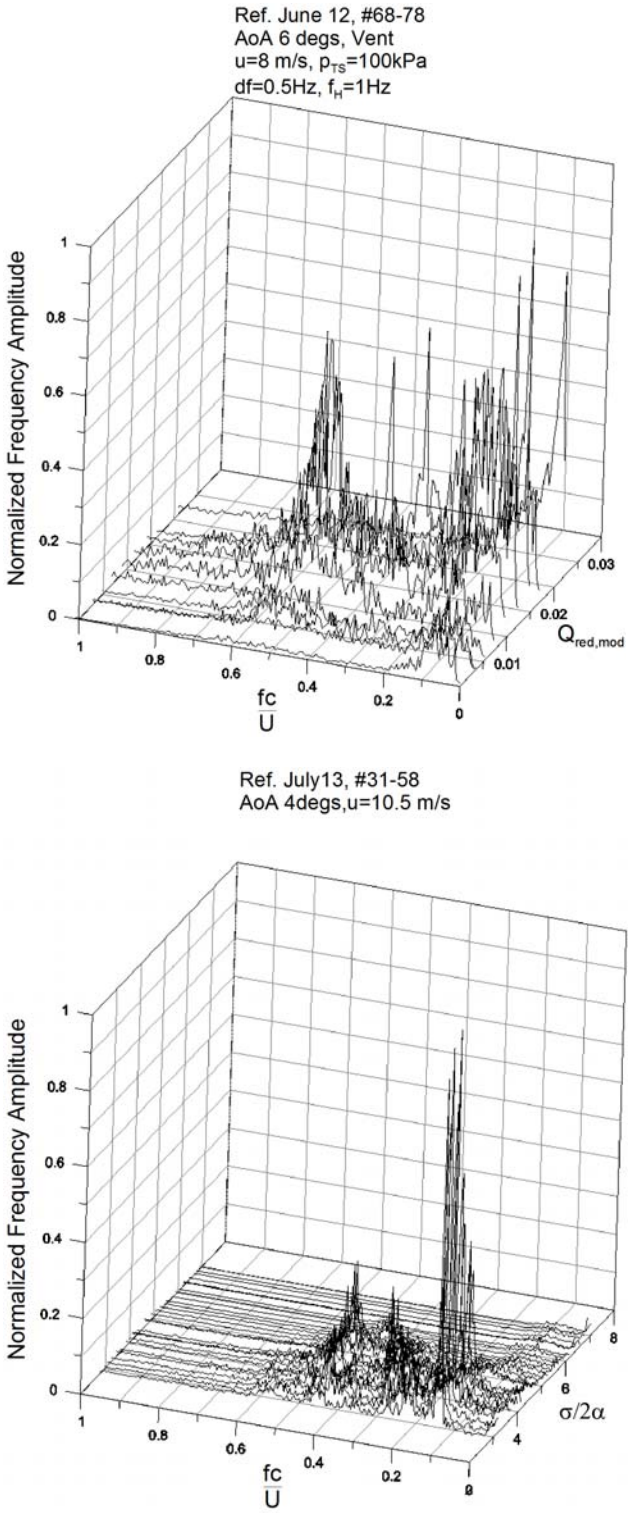

Figure 9: Spectral content of dynamics for ventilated flows (above) and cavitation flow (below). Lift measurements data for ventilated conditions (above) have been hi-pass filtered at f_H=1 Hz, corresponding to $fc/U \approx 0.01$.

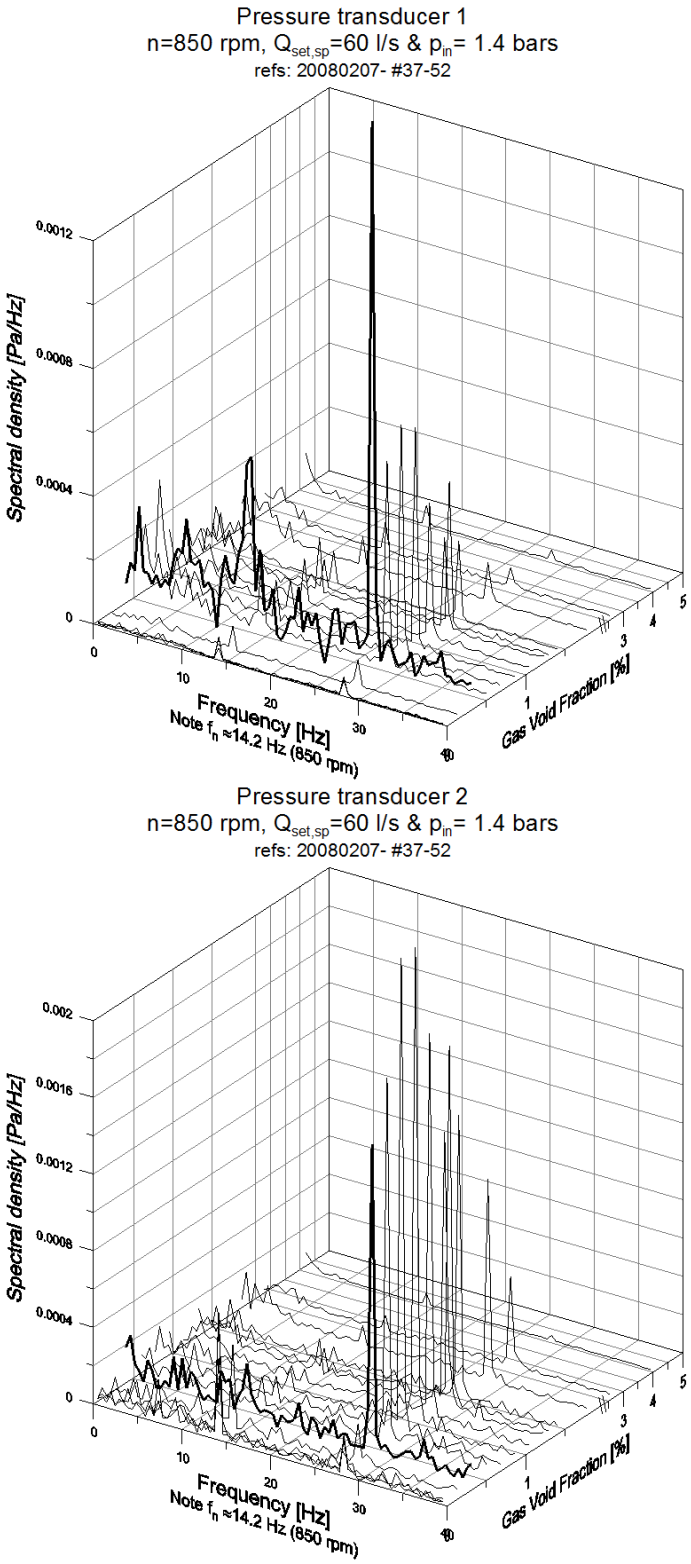

Figure 10: Spectral content of pressure dynamics measured by the two pressure transducers at the inlet section of the pump impeller. The highest spectral content for gas loaded conditions is found for 2x the rotational speed and significantly amplified compared with the 0% GVF conditions. Note that the "Gas Void Fraction" axis is broken.

DISCUSSION

The gas injection applied for the pump experiments was only made through the center injection pipe, see Figure 2. Although the presence of the acrylic pipe segment allows direct observations of the bubble field no quantitative analysis such as capturing the bubble size distribution were attempted. The cylindrical shape of the injection pipe, with associated separation regions, trapped gas in the wake in the lee-side of the pipe. Gas was eventually shed from this region, but with less control than those sheared off at the injection ports, (4) in Figure 2. Another shortcoming was that gas was unevenly injected over the axial, and vertical, length of the injection pipe. Typically this could be improved by adding internal resistance to the gas flow at each injection port. Despite the experienced deviations from ideal injection an apparent homogeneous distribution of the bubbles was observed.

A striking similarity between cavitation and gas loading was observed for the hydrofoil, Figure 4. This similarity is achieved when the cavitation index and the ventilated cavity index (as defined herein) takes a similar value. Visual inspection of the two flows also suggests a similarity. Figure 5 indicates that the performance is little dependent on gas- water density ratios, though it should be kept in mind that a small range has been investigated. When observing the spectrum characteristics of the two flows, see Figure 9, a difference is present. The defined spectral frequencies for a cavitating hydrofoil, as has been discussed previously by the authors see e.g. Kjeldsen et al [3], are not found for the gas loaded hydrofoil. Instead a lower frequency activity is observed.

The pump experiments confirms that a moderate gas load induces the higher oscillations, see Figure 7. The very same figure also suggests that the maximum oscillations are shifted to higher gas void fractions. This can very well be explained by that the lower operation locally have a lower cavitation- or, here, ventilated cavity index due to higher incident angles. Figure 8 suggests that, as with the hydrofoil, the dynamics is little dependent on the gas-water density ratios. Again a small range of pressures have been investigated. It should also be noted that the discrepancies in unsteady levels at higher gas void fraction is yet to be addressed. The spectrum analysis, see Figure 10, challenges the similarity between the hydrofoil and the pump behavior. The dominating frequency, when oscillations levels are at a maximum, is two times the rotational frequency of the pump. At this point it's natural to draw the attention to the cross bar at the pump inlet, see Figure 3. Two hypotheses can be launched:

1. The wake, or wake shedding, behind the cross bar is strongly dependent on the gas void fraction.
2. The impeller blade shedding dynamics is being locked by the perturbation of the cross bar.

The first hypothesis can't explain the apparent shift in maximum dynamics for increased flow rates, although a change in velocity over the cross bar will appear for the different operation points. The second hypothesis should be tested for the simple hydrofoil, i.e. whether small or larger upstream perturbations could lock shedding behavior.

CONCLUSION

A comprehensive experimental research program has been completed. It's shown that gas loaded and cavitating hydrofoil dynamics show striking similarities. For the hydrofoil this similarity is achieved by maintaining equal cavitation- and ventilated cavity index (as defined herein). A difference in spectral dynamics is observed.

The pressure dynamics on the impeller blade of a pump has been tested for various operation points and gas void fractions. Similarities with the hydrofoil dynamics have been observed. For the pump tested the presence of the cross-bar at the inlet of the pump is believed to determine the outcome of impeller blade dynamics.

Both systems tested suggest that pressure dynamics and hence load oscillations can be present in gas loaded systems as is observed in cavitation systems. This is a design issue that needs to be addressed especially for liquid handling systems operating with (the possibility of) gas contaminations, e.g. hydro-carbon systems.

ACKNOWLEDGMENTS

The experiments were supported by the Norwegian Research Council (Forskningsrådet) under the program "Petromaks", Flow Design Bureau AS (FDB) and Shell Technology Norway AS. One of the authors (MK) was employed by FDB during most of the periods when the experimental work took place.

NOMENCLATURE

AoA, α	= Hydrofoil angle of attack
c	= Chord length, here c=0.081m
c_L	= Lift coefficient
$c_{L,rms}$	= Standard deviation of lift coefficient time series
$c_{L,theo}$	= $2\pi\alpha$, flat plate lift coefficient
D_{max}	= Maximum bubble diameter (pump- bubble injection)
f	= Frequency
GVF	= Gas Void Fraction [%]. $GVF=Q_{gas}/Q_{Tot}$
M	= Gas mass flow rate into cavity
M	= Measured torque on pump shaft
N_{exit}	= Number of exits in bubble injection device
p_{cav}	= (Ventilated) cavity pressure
p_{ref}	= Test section reference pressure
p_{TS}	= See p_{ref}
p_{vap}	= Vapor pressure (thermodynamic prop.)
Q_{gas}	= Flow rate of gas through pump unit
$Q_{gas,injec}$	= Injected gas flow rate per exit (pump- bubble injection).
Q_{mod}	= Gas injection volumetric flow rate (hydrofoil)
$Q_{red,mod}$	= Reduced flow rate $= Q_{\mathrm{mod}} / U_{ref} c^2$ (hydrofoil)
Q_{tot}	= Total flow rate through pump $Q_{tot}=Q_{gas}+Q_w$
Q_w	= Flow rate of water /liquid through pump unit
U_{liq}	= Liquid velocity around bubble injection cylinders
U_{ref}	= Test section reference velocity
Δp	= Measured head [Pa] over pump unit.
η	= Pump efficiency
ρ	= Density

σ = Cavitation index $= \left(p_{ref} - p_{vap}\right) \Big/ 0.5U_{ref}^2 \rho_{liq}$

= Ventilated cavity index

σ_{vent} $= \left(p_{ref} - p_{cav}\right) \Big/ 0.5U_{ref}^2 \rho_{liq}$

ω = Rotational speed [rad/s] of pump

Note on measurement of hydrofoil air injection flow rate Q_{mod}/ $Q_{red,mod}$

The rotameter (Omega FL114) is calibrated for air at Standard Temperature and Pressure (STP). The parameter of interest is the flow rate through the injection slit on the hydrofoil. In order to determine that quantity the following calculations were made:

The mass flow rates, *M*, through the slit and the rotameter are similar:

$$M = \rho_{rot} Q_2 = \rho_{cav} Q_{\mathrm{mod}}$$
$$\Downarrow \rho = const \cdot p$$
$$Q_{\mathrm{mod}} = \frac{p_{rot} Q_2}{p_{cav}} = \frac{\sqrt{p_1 p_{rot}}}{p_{cav}} Q_{meas}$$

Q_{meas} is the flow rate measured as if the air was at STP, p_1 is equal to 1 atmosphere while p_{rot} is the air – pressure at the inlet of the rotameter. Now for the actual measurements only a limited set contained both the cavity, p_{cav}, and the rotameter pressure, p_{rot}, while all measurements contained the cavity pressure, p_{cav}. In order to determine Q_{mod} with limited pressure information a momentum analysis is made. The pressure drop for a compressible medium can be expressed as:

$$\Delta p = f \frac{\Delta x}{D} \rho(p) U^2$$
$$\Downarrow U = \frac{M}{\rho A}, \rho = const \cdot p$$
$$\Delta p = f \frac{1}{D} \frac{M^2}{A^2} \frac{1}{p \cdot const} \Delta x$$
$$\Rightarrow \int_{p_{cav}}^{p_{tot}} p dp = \int_0^L f \frac{1}{D} \frac{M^2}{A^2} \frac{dx}{const}$$
$$\Rightarrow p_{rot}^2 - p_{cav}^2 = M^2 \cdot const$$

Replacing the mass flow rate, *M*, with the relation above we find:

$$p_{rot}^2 - p_{cav}^2 = M^2 \cdot const = \rho_{cav}^2 Q_{\mathrm{mod}}^2$$
$$\Downarrow Q_{\mathrm{mod}} = \frac{\sqrt{p_1 p_{rot}}}{p_{cav}} Q_{meas} \ and \ \rho_{cav} = const. \cdot p_{cav}$$
$$p_{rot}^2 - p_{cav}^2 = const \cdot p_1 p_{rot} Q_{meas}^2$$

Using the set of experiments containing both p_{cav} and p_{rot} the constant can be determined, and once that is known the pressure at the rotameter inlet can be found through the latter equation. Now some scatter is present while determining the constant as can be seen below.

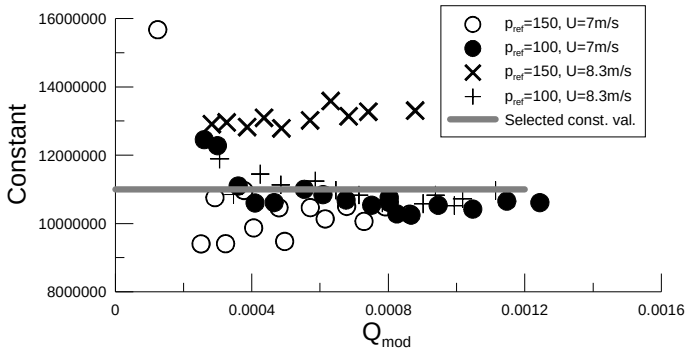

Figure depicts scatter in determining constant used for quantifying injection flow rate.

REFERENCES

[1] Kjeldsen, M and Arndt, R.E. A *On similarities between flow systems operating at excessive gas load and at cavitation conditions: hydrofoil tests and cfd assessment* The 12th International Symposium on Transport Phenomena and Dynamics of Rotating Machinery Honolulu, Hawaii, February 17-22, 2008

[2] Silberman, E. 1957 *Production of Bubbles by the Disintegration of Gas Jets in Liquids SAFL Technical Paper* no 12 Series A. Reprinted from Fifth Midwestern Conference on Fluid Mechanics, 1957: Gas Jets in Liquids

[3] Kjeldsen, M Arndt, R.E.A. & Effertz, M. *Spectral Characteristics of Sheet/Cloud Cavitation* ASME Journal of Fluids Engineering Sept 2000, Vol. 122, pp.481-487

[4] Amromin EL, Kopriva J, Arndt REA & Wosnik M *Hydrofoil Drag Reduction by Partial Cavitation* ASME Journal of Fluids Engineering Sept 2006, Vol. 128, pp. 931-936

[5] English, JW *Air Injection as a Means of Reducing Propeller Cavitation Induced Ship Vibration* Proceeding pp.253-257 3rd Int Symp on Cavitation, April 1998, Grenoble, France.